
This is the Accepted version of the article

Automatic Intraoperative Correction of Brain Shift for Accurate Neuronavigation

Daniel Høyer Iversen, Wolfgang Wein, Frank Lindseth, Geirmund Unsgård, Ingerid Reinertsen

Citation:

Daniel Høyer Iversen, Wolfgang Wein, Frank Lindseth, Geirmund Unsgård, Ingerid Reinertsen (2018)
Automatic Intraoperative Correction of Brain Shift for Accurate Neuronavigation, World Neurosurgery
120, e1071-e1078. DOI: 10.1016/j.wneu.2018.09.012

This is the Accepted version.
It may contain differences from the journal's pdf version

This file was downloaded from SINTEFs Open Archive, the institutional repository at SINTEF
<http://brage.bibsys.no/sintef>

Automatic intra-operative correction of brain-shift for accurate neuro-navigation

Daniel Høyer Iversen (MSc, PhD)^{1,2}, Wolfgang Wein (MSc, PhD)³, Frank Lindseth (MSc, PhD)^{4,1}, Geirmund Unsgård (MD, PhD)^{5,6}, Ingerid Reinertsen (MSc, PhD)¹

¹ SINTEF Technology and Society, Dept. Health Research, Trondheim, Norway

² Dept. Circulation and Medical Imaging, Norwegian University for Science and Technology (NTNU), Trondheim, Norway

³ ImFusion GmbH, Munchen, Germany

⁴ Dept. of Computer Science, Norwegian University for Science and Technology (NTNU), Trondheim, Norway

⁵ Dept. Neurosurgery, St. Olav University Hospital, Trondheim, Norway

⁶ Dept. of Neuromedicine and Movement Science, Norwegian University for Science and Technology (NTNU), Trondheim, Norway

Corresponding author:

Ingerid Reinertsen
SINTEF Technology and Society, Dept. Health Research
P. B. 4760 Torgard
7465 Trondheim
Norway
Email: Ingerid.Reinertsen@sintef.no

Abstract

Background: Unreliable neuro-navigation due to inaccurate patient-to-image registration and brain-shift is a major problem in conventional MR guided neurosurgery.

Objective: Perform a prospective intra-operative validation of a system for fully automatic correction of this inaccuracy based on intra-operative 3D ultrasound (US) and MR-to-US registration.

Methods: The system has been tested intra-operatively in thirteen tumor resection cases and the performance has been evaluated intra-operatively and post-operatively.

Results: Intra-operatively, the system was evaluated to be accurate enough for tumor resection guidance in 9 of 13 cases. Manually placed anatomical landmarks showed an improvement of the alignment from 5.12 mm to 2.72 mm (median) after intra-operative correction. Post-operatively, the limitations of the current system were identified and modified for the system to be sufficiently accurate in all cases.

Conclusion: We have shown that automatic and accurate correction of spatially unreliable neuro-navigation is feasible within the constraints of surgery. We have also identified and addressed the current limitations of the system.

Keywords: Brain shift, Neuronavigation, MRI, Ultrasound

1. Introduction

Accurate mapping between pre-operative MR images and the patient is key to reliable neuro-navigation. This mapping is often established using fiducial markers, anatomical landmarks, surface points or a combination of these. The accuracy of this initial mapping is limited by possible movement of markers, movement of skin and inaccurate sampling of points or surfaces. Still, this mapping is usually sufficiently accurate for positioning the patient's head and planning the craniotomy. Opening the skull and dura will result in brain-shift due to leakage of cerebrospinal fluid (CSF), gravity and administration of drugs. A thorough review of the extent and causes of brain-shift was presented by Gerard et al¹. Both inaccurate image-to-patient registration and brain-shift contribute to unreliable neuro-navigation, and the pre-operative MR images can thus no longer be trusted for resection guidance. To correct for these effects, intra-operative imaging is an attractive solution. Intra-operative MR imaging can provide decent

quality images and has the advantage of full head coverage. However, the image quality is lower than in conventional pre-operative MR imaging, and the high cost combined with the need for specially adapted operating rooms limits the widespread use of this solution. Furthermore, the time requirements for scanning often limit the use to a single scan towards the end of surgery. Intra-operative ultrasound on the other hand presents several advantages in this context. Ultrasound is cheap, portable, provides real time imaging and is available in most neurosurgical departments. Commercial neuro-navigation systems that support intraoperative ultrasound imaging include the widely used BrainLab and Medtronic systems.

In general, navigated intra-operative ultrasound images are acquired directly in the patient frame of reference using a tracked ultrasound probe. Consequently, the spatial accuracy of the ultrasound images is independent of the initial mapping between MR images and the patient. The overall navigation accuracy using a recently acquired 3D ultrasound volume has been shown to be less than 2mm². However, the interpretation of the ultrasound images may present an important obstacle in the efficient use of this modality. Proper and dedicated training of neurosurgeons in ultrasound anatomy of the brain is needed. To take full advantage of the high quality pre-operative MR images, we propose a framework for intra-operative correction of the pre-operative MR volumes based on intra-operative ultrasound. Using MR-to-ultrasound image registration the MR images can be corrected for inaccuracies due to initial mapping and brain-shift and thus be updated according to the current surgical situation. Following this MR-to-US registration, the MR images can be trusted and used actively during tumor resection. This can be particularly important in cases where the tumor borders are diffuse and difficult to assess in the ultrasound images. Several methods for MR-to-ultrasound registration have been proposed over the last years. De Nigris et al.³ proposed a method based on alignment of gradient orientations and validated their method on retrospective data. Rivaz et al.⁴ introduced a patch-based correlation ratio technique to perform deformable registration of the same retrospective data⁵. Methods for correction of brain-shift using biomechanical models have been proposed by Chen et al.⁶ and Morin et al.⁷. None of these methods have been tested and evaluated in the operating room by neurosurgeons.

In our previous work, we have presented the use of a vessel based method for intra-operative correction of brain shift⁸. While this method produced accurate results in cases where corresponding vessels could be imaged both with MR angiography (MRA) and power Doppler

ultrasound, some important limitations remained. First, the method requires pre-operative MRA which is not part of the standard imaging protocol for brain tumor surgery. Second, imaging of corresponding vessels is not trivial as the vessels most easily imaged with MRA (major vessels close to the skull base) are often located too deep for high quality ultrasound imaging and are not significantly affected by brain-shift. Vessels close to the surface are more easily imaged with power Doppler ultrasound, but often invisible in MR angiography. In addition, vessel segmentation and centerline extraction add to the processing steps and computation time intra-operatively. To address these limitations and have a fully automatic setup, we combined the open-source intra-operative navigation platform CustusX⁹ with the commercially available image registration software ImFusion Suite (ImFusion GmbH, Munich, Germany) to test the hypothesis that correction for brain-shift can be automatically performed in the operating room during surgery and be accurate enough for brain tumor resection guidance. We have tested the method intra-operatively in 13 cases of gliomas resection. The results were evaluated both intra-operatively and post-operatively.

2. Methods

2.1 Patients and pre-operative MR data

Thirteen patients with primary or recurring gliomas were prospectively included in the study. Patient selection was based on availability of personnel and equipment rather than patient characteristics. The study was approved by the Regional committee for medical and health research ethics and all patients provided written informed consent. Patient characteristics are detailed in Table 1.

Pre-operative MR data were acquired the day before surgery and included Gd-enhanced T1 weighted images and FLAIR images, both with 256x256x192 voxels and a voxel size of 1 mm³. These MR sequences are part of the routine clinical preparations for brain tumor surgery. Following the fixation of the patient's head in the Mayfield clamp on the operating table, the pre-operative MR images were registered to the patient using five fiducial markers glued to the skin prior to MR imaging. However, for patient #10 anatomical points (eyes, ears, nasion) were used instead of fiducials. In all cases, except for patient #8, 10 and 12 where Gd-enhanced MR T1 were used, pre-operative MR FLAIR were registered to the first B-mode acquisition acquired before any resection.

2.2 Intraoperative setup and workflow

The intraoperative setup used in the operating room is shown in Figure 1. The research neuro-navigation system was run in parallel with the commercial system (Sonowand Invite, Sonowand AS, Trondheim, Norway). The research system consisted of a navigation rack with our open-source platform CustusX⁹. The navigation system was connected to an optical position tracker (NDI Polaris Spectra; Northern Digital, Waterloo, Canada) and a GE Vingmed E9 ultrasound scanner with a GE 11L linear array transducer (GE Vingmed Ultrasound, Horten, Norway). The optical tracker was used to acquire the position and orientation of the ultrasound probe and surgical tools including the navigation pointer, ultrasonic aspirator and the biopsy forceps. All navigated tools were visualized relative to both pre-operative and intra-operative images on the navigation screen. A screenshot from the navigation system is shown in Figure 2. Two-dimensional (2D) ultrasound images were obtained by free-hand scanning over the region of interest. The ultrasound scanner transmitted 2D ultrasound frames to the navigation system via a digital research interface and the position and orientation of each 2D frame were stored during acquisition. Further, three-dimensional (3D) ultrasound volumes were generated by reconstructing the 2D ultrasound frames into a single volume¹⁰. Following 3D reconstruction, the pre-operative MR images were automatically registered to the newly acquired US volume using the registration method described in Section 2.3 The image registration software was run as an independent package called from the navigation system interface, and the result was automatically loaded in the navigation system.

2.3 Registration method

An image-based registration algorithm^{11,12}, which is part of the ImFusion Suite software environment, is used in this study. At its core is a similarity measure which assesses the alignment of 3D ultrasound and MR volumes directly using statistics on the voxel intensities within 3D-patch neighborhoods. It is therefore invariant to the brightness and contrast of anatomical structures throughout the data set. More importantly, the used model allows a correlation of ultrasound intensities to both MR intensities or their border structures (gradients), respectively. This is an important physical consideration when dealing with ultrasound image data, since strong echoes might either correspond to hyperechoic tissue, or borders between

different anatomical structures. As opposed to related intensity-based algorithms that use a higher abstraction from the intensities such as gradients¹³ or self-similarity¹⁴, this method is hence able to utilize more of the original image data throughout the volumes. This similarity measure is evaluated repeatedly while re-sampling the MR data with a different transformation, where a non-linear optimization algorithm optimizes its value with respect to the rigid transformation parameters. The initial transformation parameters are given by the tracked neurosurgical setup, and the optimization terminates once the similarity measure does not improve any more up to a numerical limit. The final result of the algorithm is hence a transformed pre-operative MR scan aligning well with the intra-operative US scan and the live patient anatomy.

2.4 Evaluation of registration accuracy

2.4.1 Evaluation of intra-operative results

Immediately following image registration, the surgeon performed an evaluation of the registration result and decided whether the result was accurate enough for guidance of the resection. *The neurosurgeon identified a structure of interest such as a sulcus or the wall of a ventricle in the ultrasound image with the virtual extension of the navigated pointer (“offset”).* We then used the “registration history” feature in CustusX that enables easy toggling between the “before registration” and “after registration” while the surgeon evaluated the correspondence between the MR images and, the ultrasound image and the patient using the navigated pointer. This procedure was repeated for several structures for each patient until the surgeon felt that he had sufficiently examined the quality of the registration. Screenshots from the navigation system illustrating this feature are shown in Figure 3. All included patients were operated by the same surgeon (GU).

If the registration was judged insufficient for resection guidance, the resection was guided by the ultrasound volume alone. The surgeon did not evaluate the standard neuronavigation in this context. Post-operatively, the intra-operative registration results were evaluated by placing ten homologous anatomical landmarks in the MR and ultrasound image volumes and computing the Euclidean distance between points before and after registration. A Wilcoxon test for paired samples was used to compare the landmark distances before and after intra-operative rigid registration.

2.4.2 Retrospective optimization of the registration pipeline

We considered the cases where intra-operative registration was defined insufficient, and optimized the registration algorithm to succeed on those cases as well. Improvements included parameter tuning of the similarity measure, changing the optimization scheme for increased capture range in case with large initial displacement, and using different transformation models in certain cases. To assess the precision, i.e. the repeatability with which the automatic brain-shift correction finds the same results, we have performed a study where we randomly perturbed the landmark-based reference registrations. We translated the MRI between 0 and 20 mm in x, y and z directions and rotated between 0 and 20 degrees around each axis. The registration algorithm was executed from 100 such randomly perturbed starting positions for each of the patient data sets. We then separated wrong registrations (outliers) from correctly converged results. This retrospective evaluation is required in order to obtain the likelihood of an accurate brain-shift correction given different imaging circumstances, initial errors, and actual patient anatomy. Wilcoxon tests for paired samples were used to compare intra-operative rigid registration versus retrospective rigid registration and retrospective rigid versus affine registration.

3. Results

3.1 Intra-operative evaluation of registration accuracy

The results of the surgeon's evaluation in each surgical case is shown in Table 2. Nine out of thirteen cases were evaluated as accurate enough for resection guidance by the surgeon immediately following registration. The corrected MR images were presented within a few minutes following ultrasound acquisition, and the surgeon evaluated the accuracy before any further tumor resection. For patient #1, there was a problem with the navigation setup in the operating room resulting in movement of the reference frame relative to the patient's head after MR-to-patient registration. Consequently, the initial misalignment was larger than the capture range of the registration algorithm. Patient #7 was a re-operation of a low-grade tumor. Consequently, there was already a considerable resection cavity present from the beginning of the procedure. After opening of the dura, there was a large surface shift with non-rigid deformation of the tissue due to leakage of CSF. The deeper structures such as the ventricles were well aligned after registration, but the rigid transformation was not able to correct for the deformation that occurred close to the surface. Patient #9 had a large craniotomy and the sinking

of the surface in the direction of gravity was considerable. The rigid registration was not able to fully recover this deformation as could be expected. Patient #10 did not have fiducial markers glued to the skin before MR scanning. MR-to-patient registration was therefore done using anatomical landmarks such as the nose and the ears. This resulted in a less accurate registration than usual and consequently a large initial misalignment. In addition, the tumor was a large and soft cystic tumor. After opening of the dura there was considerable deformation close to the surface. As for patient #7 and #9, the registration algorithm was unable to account for the deformation. The registration greatly improved the alignment, but the error was still too large for resection guidance.

Post-operatively, the intra-operative results were evaluated by placing homologous anatomical landmarks in the MR and US images. The Euclidean distances between these landmarks before and after registration are shown in Table 2. The median distance was reduced from 5.12 mm before registration to 2.72 mm after registration. Using the Wilcoxon test for paired samples, the result was statistically significant with $p=0.0047$.

3.2 Retrospective optimization of registration pipeline and robustness evaluation

The final registration results after retrospective optimization are shown in Table 3 are presented using both rigid and affine transformation models. The latter includes non-uniform scaling and shearing of the MR scan, hence compensating for some of the deformations which might have occurred intra-operatively. The column “ground truth” denotes the landmark error when the best possible rigid transformation is defined on the landmark correspondences themselves, and therefore represents the lower bound of the error that registration with a rigid transformation can achieve. Following this optimization, the median Euclidian distance between corresponding landmarks was reduced to 1.80 mm after rigid registration and 1.70 mm after affine registration. Using the Wilcoxon test for paired samples, the distances after retrospective rigid registration were significantly smaller than after intra-operative rigid registration ($p=0.0159$), and the distances after retrospective affine registration were significantly smaller than after retrospective rigid registration ($p=0.0340$).

In the retrospective evaluation of the capture range and robustness of the algorithm between 53% and 87% of the registrations succeeded, on average 71%. The maximum landmark error for the converged results was 2.87 mm on average. On 11 of the patients, the cluster of correct registrations was clearly separated from the outliers, with very little variation within those results. Patient 9 however did have a seamless transition from good to bad registration, because the recorded ultrasound volume was too large for a single rigid transformation to yield a good fit; patient 10 exhibits a cavity with structural mismatch or compression, where there was no single good alignment that could be identified as part of the randomized trial.

4 Discussion

In this paper, we have demonstrated the use of intra-operative MR-to-US registration in thirteen prospective glioma cases. We have shown that automatic intra-operative image registration for updated neuro-navigation can be sufficiently accurate for guidance of brain tumor resections and fast enough to provide results within a minute after acquisition of the ultrasound volume. The presented system is based on both open source and commercially available software, and requires no manual pre-processing of the image data such as segmentation of structures or identification of points. The cases presented include both high grade and low-grade gliomas, and both primary operations and re-operations for removal of recurrent tumor. The imaging characteristics of these tumors are difficult to predict and present significant variability. In addition to variable imaging characteristics due to heterogeneous tumors, the system could handle large anatomical variation due to previous surgeries including large resection cavities. These results are promising even though thirteen patients is not sufficient to conclude on the overall robustness of the approach.

The most important result in this context is whether the surgeon consider the registration result to be accurate enough for surgical guidance. This assessment depends obviously on the registration result, but also on the situation before registration. If the mismatch between the images was large before registration, the result after registration might still be significantly better even if the alignment is not judged perfect in all regions. As the registration used in this study was limited to a rigid transformation intra-operatively, there were cases where the method was unable to fully recover the mismatch. For the surgeon to trust the registration result, the visual

assessment of the alignment between the images is essential. We argue that the visual feedback is as powerful as a quantitative error measure in this context. In the navigation platform CustusX, this issue is solved with the “registration history” feature which makes it possible to toggle between the different registration steps and visualize the corresponding images. We find this feature indispensable for intra-operative evaluation of the registration results.

In four patients, the intra-operative registration failed to produce accurate results in its first version. In patient #1, the initial misalignment was larger than the capture range of the registration algorithm. This issue was corrected in the post-operative optimization and resulted in greatly improved results. For patients #7, #9 and #10 there were large surface shifts with considerable non-rigid deformation. As expected, the rigid transformation was not able to correct for this deformation. The distance between manually placed anatomical landmarks in the two images to be registered is a widely used error metric. However, in patient #7, there was a large cavity from an earlier procedure. As the region of the cavity didn't have any features suitable for reliable anatomical landmarks, the failure to correct for the deformation close to the surface is not well reflected by the landmark error measure. This situation is shown in Figure 4, where the region closer to the surface is subject to larger deformation than the deeper regions.

The quantitative evaluation using homologous anatomical landmarks show results comparable to ¹¹ and ¹². As stated in ¹², applying deformable registration to a mainly rigid misalignment will not improve the accuracy. However, patients #7 and #10 present considerable deformation due to very soft tumor tissue, and in these cases deformable registration would be helpful. Post-operatively, the registration pipeline was optimized to produce accurate results in all cases. Homologous landmarks identified in MR and ultrasound were used to quantify the registration error. Landmarks are widely used in the literature to validate registration results as an approximation of the ground truth^{4,3,5,15}. In patient #7 the registration error as measured with homologous landmarks is 1.94 mm. This shows that the alignment of the features in the images is good after registration. Close to the surface, however, there are few reliable landmarks and the misalignment in this region is not well captured by the landmark metric. In an additional robustness study, 71% of registrations succeeded from far displaced initializations with very good precision in 11 out of the 13 patients, which suggests a high likelihood that the method will succeed in general in arbitrary surgical scenarios.

The rigid registration presented in this study improves the alignment of the MR and ultrasound image volumes, but as brain shift is a highly non-linear process, affine and fully deformable registration have the potential to further improve the results. Newer versions of the registration software include both affine and fully deformable registration, which could greatly improve the accuracy in some of the cases presented here. Future developments will also include registration after the resection has started considering the resected tissue, more complex deformations and the resection cavity. Accurate registration throughout surgery will be needed in order to have a fully functional and useful tool for resection guidance. More extensive testing and validation is also required, ideally as part of a commercial neuronavigation system with ultrasound capabilities.

5 Conclusion

In summary, accuracy, robustness and computation time of the used automatic preoperative MR to intraoperative US registration algorithm, can be regarded as acceptable for regular clinical use, and therefore greatly increase the accuracy of neuro-navigation after opening the dura. . The registration does not require any user interaction, and was retrospectively improved to succeed on all presented cases. Nevertheless, it is still mandatory to have a validation step where the surgeon visually assesses the quality of the alignment after registration, because due to the dependence of the algorithm on anatomical structures, it might be impossible to ever perform a full proof that the method would always succeed in general. To further increase the value of intra-operative algorithms, the presented software algorithms should be further extended to allow for a regular registration even during and after resection. This comes with the additional challenge of having to distinguish resected areas (which should not be subject to a re-alignment) from anatomical regions which should still match to the pre-operative MRI. Using combinations of advanced segmentation, classification and image-based registration methodology, such automatic algorithms are however in reach. They could lead to even more confidence in the resected anatomy and therefore smaller safety margins and tumor recurrence.

Aknowledgements/Funding: D. H. I. received funding from the *Liaison Committee between the Central Norway Regional Health Authority (RHA) and the Norwegian University of*

Science and Technology (NTNU). This work was supported by the *Norwegian National Advisory Unit for Ultrasound and Image Guided Therapy*.

References

1. Gerard IJ, Kersten-Oertel M, Petrecca K, Sirhan D, Hall JA, Collins DL. Brain shift in neuronavigation of brain tumors: A review. *Med Image Anal.* 2017;35:403-420. doi:http://dx.doi.org/10.1016/j.media.2016.08.007.
2. Lindseth F, Lango T, Bang J, Nagelhus Hernes TA. Accuracy evaluation of a 3D ultrasound-based neuronavigation system. *Comput Aided Surg.* 2002;7(4):197-222.
3. De Nigris D, Collins DL, Arbel T. Multi-modal image registration based on gradient orientations of minimal uncertainty. *IEEE Trans Med Imaging.* 2012;31(12):2343-2354. doi:10.1109/TMI.2012.2218116.
4. Rivaz H, Chen SJ-S, Collins DL. Automatic Deformable MR-Ultrasound Registration for Image-Guided Neurosurgery. *IEEE Trans Med Imaging.* 2015;34(2):366-380. doi:10.1109/TMI.2014.2354352.
5. Mercier L, Del Maestro RF, Petrecca K, Araujo D, Haegelen C, Collins DL. Online database of clinical MR and ultrasound images of brain tumors. *Med Phys.* 2012;39(2012):3253. doi:10.1118/1.4709600.
6. Chen I, Coffey AM, Ding S, et al. Intraoperative brain shift compensation: Accounting for dural septa. *IEEE Trans Biomed Eng.* 2011;58(3 PART 1):499-508. doi:10.1109/TBME.2010.2093896.
7. Morin F, Courtecuisse H, Reinertsen I, et al. Brain-shift compensation using intraoperative ultrasound and constraint-based biomechanical simulation. *Med Image Anal.* 2017;40. doi:10.1016/j.media.2017.06.003.
8. Reinertsen I, Lindseth F, Askeland C, Iversen DH, Unsgård G. Intra-operative correction of brain-shift. *Acta Neurochir (Wien).* 2014;156(7):1301-1310.
9. Askeland C, Vegard O, Janne S, et al. CustusX : an open-source research platform for image-guided therapy. 2015. doi:10.1007/s11548-015-1292-0.
10. Øygaard T. Improved Distance Weighted GPU-based 3D Ultrasound Reconstruction

- Methods. *Masters thesis, NTNU*. 2014;(February). doi:10.1007/978-90-481-9082-9_1.
11. Wein W, Ladikos A, Fuerst B, Shah A, Sharma K, Navab N. Global registration of ultrasound to MRI using the LC2 metric for enabling neurosurgical guidance. *Med Image Comput Comput Assist Interv*. 2013;16(Pt 1):34-41.
 12. Fuerst B, Wein W, Muller M, Navab N. Automatic ultrasound-MRI registration for neurosurgery using the 2D and 3D LC(2) Metric. *Med Image Anal*. 2014;18(8):1312-1319.
 13. De Nigris D, Collins D, Arbel T, Nigris D De. Fast and Robust Registration Based on Gradient Orientations: Case Study Matching Intra-Operative Ultrasound to Pre-Operative MRI in Neurosurgery. *Ipcai*. 2012:125-134. http://link.springer.com/chapter/10.1007/978-3-642-30618-1_13.
 14. Heinrich MP, Jenkinson M, Bhushan M, et al. MIND: Modality independent neighbourhood descriptor for multi-modal deformable registration. *Med Image Anal*. 2012;16(7):1423-1435. doi:10.1016/j.media.2012.05.008.
 15. Xiao Y, Fortin M, Unsgård G, Rivaz H, Reinertsen I. RETroSpective Evaluation of Cerebral Tumors (RESECT): A clinical database of pre-operative MRI and intra-operative ultrasound in low-grade glioma surgeries: A. *Med Phys*. 2017;44(7). doi:10.1002/mp.12268.

Figure legends:

Figure 1: The experimental setup in the operating room showing the research rack with the navigation software, the ultrasound scanner and the commercial neuronavigation system Sonowand Invite.

Figure 2: Screenshot from the navigation system CustusX showing a 3D rendering of the pre-operative MRI and the navigation pointer (left), axial/coronal/sagittal slices of the pre-operative MRI FLAIR (middle) and axial/coronal/sagittal slices of the intra-operative ultrasound volume (right).

Figure 3: Screenshots from the navigation system illustrating the toggling between the situation before registration (left) and after registration (right). If the situation shown in the display panels is not the current situation, the registration history button is red to warn the user (see the red circle in the top middle of the screenshots). This feature enables easy visual evaluation of the registration result.

Figure 4: Example of two landmarks in the same patient that experience different types of brain-shift. Left: Example of a landmark close to resection cavity (point A) that is subject to large deformation and where rigid registration alone is unable to recover the misalignment. Right:

Example of a landmark (point B) where the rigid registration is successful in correcting the misalignment.

Patient no	Tumor type	Anatomical location	Re-operation/primary
1	HGG	Right parietal lobe	Primary
2	HGG	Right insula	Re-operation
3	LGG	Left frontal lobe	Primary
4	HGG	Left temporal lobe	Re-operation
5	LGG	Right temporal lobe	Re-operation
6	HGG	Right insula	Re-operation
7	LGG	Left frontal lobe	Re-operation
8	LGG	Right frontal lobe	Re-operation
9	LGG	Right frontal lobe	Primary
10	HGG	Left temporal lobe	Primary
11	HGG	Left frontal/parietal lobe	Primary
12	HGG	Right limbic/parietal lobe	Primary
13	LGG	Left insula	Re-operation

Table 1: Patient data (HGG: High-grade glioma, WHO grade III or IV, LGG: Low-grade glioma, WHO grade II)

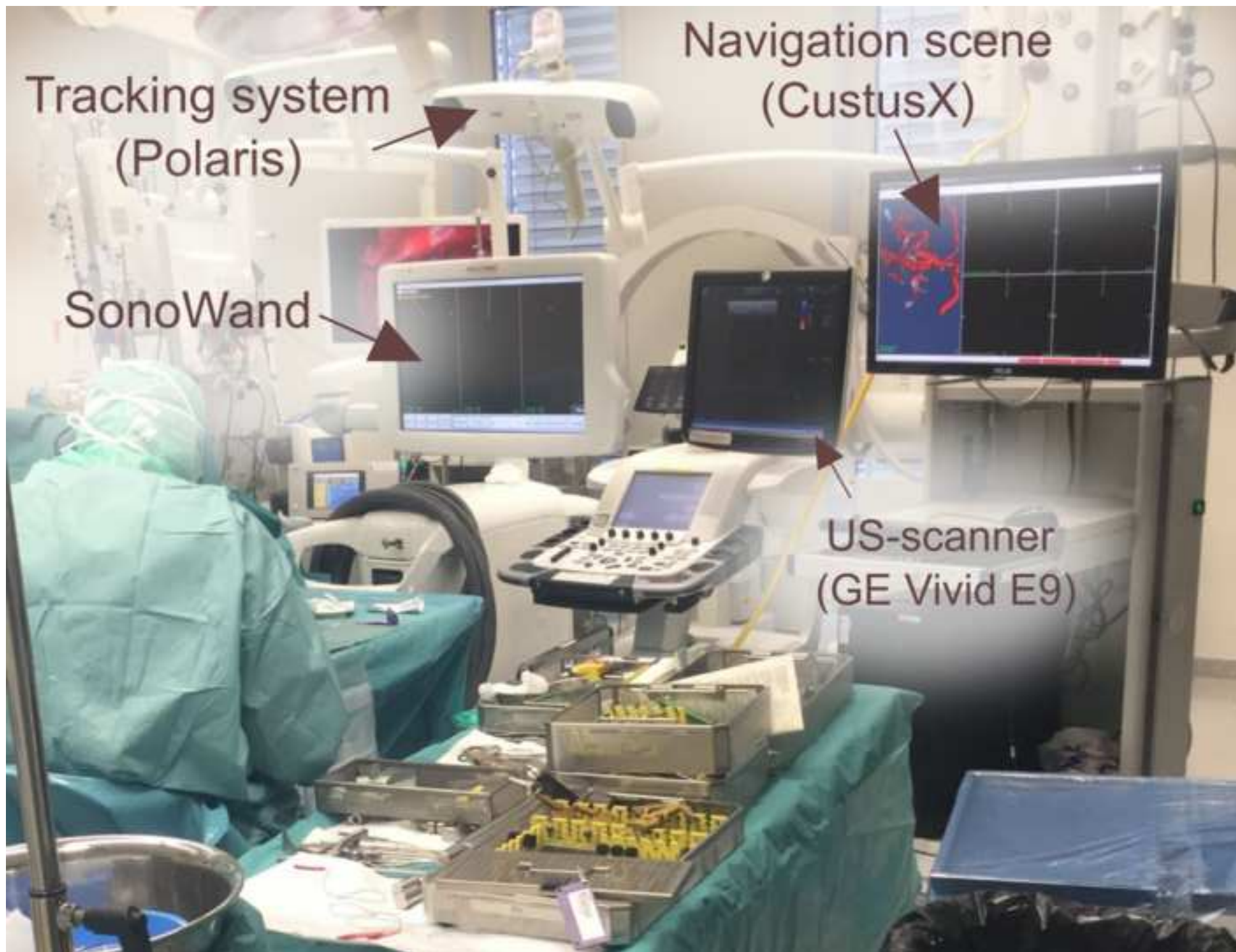
Patient no	Intra-op success	Before(mm)	After(mm)
1	No	23.30	18.47
2	Yes	4.82	3.40
3	Yes	10.19	2.74
4	Yes	5.83	3.66
5	Yes	10.24	2.05
6	Yes	5.12	1.97
7	No	5.24	1.97
8	Yes	4.02	2.72
9	No	4.73	6.33
10	No	17.53	9.31
11	Yes	4.02	1.93
12	Yes	2.52	2.09
13	Yes	2.65	1.52
Mean		7.71	4.47
Median		5.12	2.72

Table 2: Intra-operative evaluation of success and distances (mm) between landmarks before and after image registration.

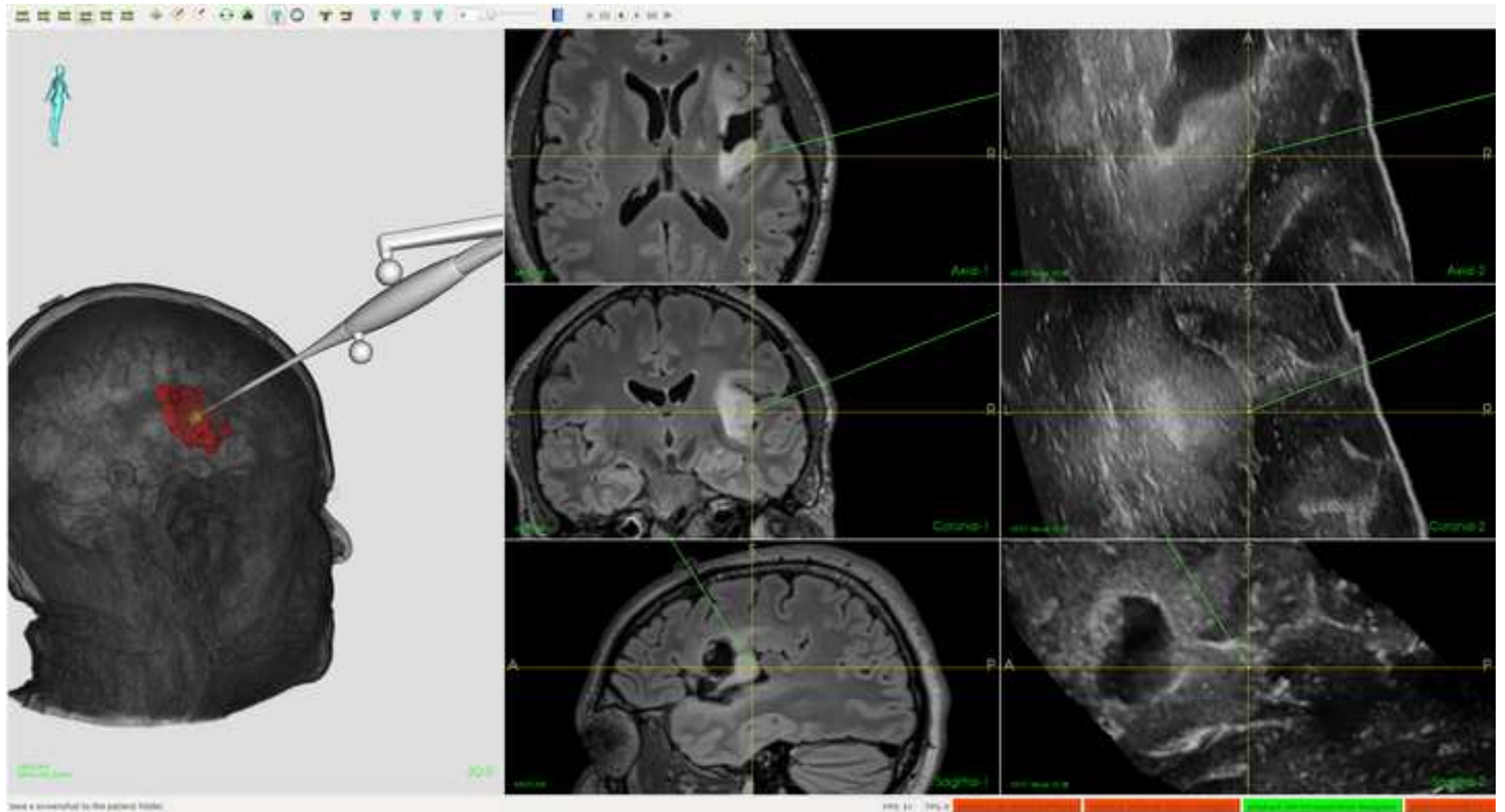
Patient no	Before	Rigid (IO)	Rigid (RO)	Affine (RO)	Ground truth
1	23.30	18.47	5.90	4.90	5.40
2	4.82	3.40	3.80	2.20	2.30
3	10.19	2.74	1.70	1.20	1.50
4	5.83	3.66	1.80	2.50	1.50
5	10.24	2.05	2.30	2.30	1.80
6	5.12	1.97	1.90	1.50	1.30
7	5.24	1.97	1.50	1.70	1.30
8	4.02	2.72	1.80	1.70	1.70
9	4.73	6.33	3.70	2.60	3.10
10	17.53	9.31	5.60	5.40	2.40
11	4.02	1.93	1.60	1.30	1.30
12	2.52	2.09	1.70	1.40	1.50
13	2.65	1.52	1.80	1.50	1.20
Mean	7.71	4.47	2.70	2.32	2.02
Median	5.12	2.72	1.80	1.70	1.50

Table 3: Distances (mm) before and after intraoperative (IO) and retrospective optimization (RO) of the registration pipeline. The columns show the distance before registration, after intraoperative registration, after retrospective optimized rigid registration, after retrospective optimized affine registration and the lower bound for the rigid registration (left to right).

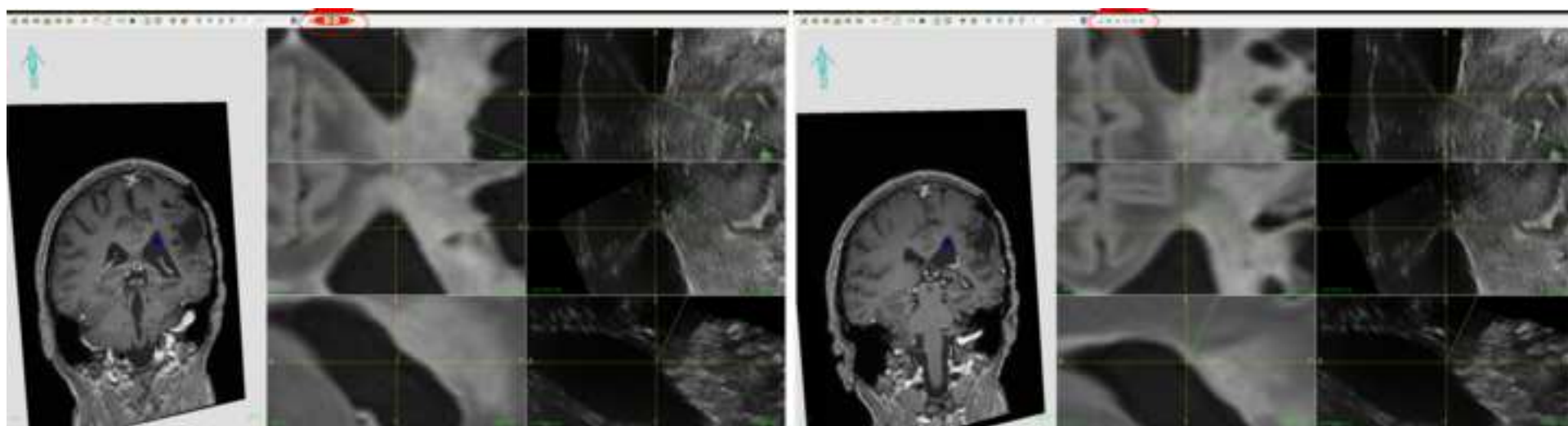
Figure(s)
[Click here to download high resolution image](#)



Figure(s)
[Click here to download high resolution image](#)



Figure(s)
[Click here to download high resolution image](#)



Figure(s)
[Click here to download high resolution image](#)

